

# A Deep Learning Method for COVID-19 Detection from X-ray Scans

Alister Luiz, Hani Ragab, Kayvan Karim and Hadj Batatia

MACS, Heriot-Watt University

## ARTICLE INFO

### Keywords:

COVID-19, SARS-CoV-2, Chest X-ray, Classification, Deep Learning, Convolutional Neural Networks

## ABSTRACT

RT-PCR is currently the most widely used diagnosis test for COVID-19. However, it has some limitations including shortage of test kits, delays in receiving results, and a relatively low accuracy of COVID-19 detection. In this paper, we propose an automated method for quick, efficient, and affordable COVID-19 diagnosis based on X-Ray scans. Our proposed method is based on a deep learning classification model for identifying lung patterns that are characteristic of COVID-19 infection.

In contrast to existing methods, we adopt a DenseNet121 architecture. We used transfer learning from an existing model to speed up the training phase. We used a dataset of a total size of 1716 X-ray scans that we did split into eleven folds. Ten folds were used in 10-fold cross validation training and testing, whereas the eleventh fold was kept aside and only used to choose the best out of the ten models produced by the 10-fold cross validation. The dataset contained 572 samples of each of the three classes: COVID-19, Pneumonia, and Negatives.

We obtained 94.6% accuracy with excellent sensitivity, specificity and F1-score for the three classes. Our method gives better diagnosis when compared with the RT-PCR test results. Further, we did implement a CNN-based model and DenseNet121 provided better results. We deployed an experimental web application ([www.aiinnov.com](http://www.aiinnov.com)) to allow live testing of our model. After thorough clinical validation, such application could help reduce workload and limit virus exposure for healthcare professionals.

## 1. Introduction

COVID-19, which was declared a global pandemic by the World Health Organization on March 11, 2020, has affected millions of people worldwide, and had important consequences on health, social life, with a severe global economic impact.

Over a billion tests have been carried across the world for diagnosing patients with COVID-19 [7]. This additional activity creates higher workload on professionals and requires complex strict organization at healthcare providers, with consequences on ordinary processes, especially for chronic diseases. Despite the ongoing vaccination efforts undertaken by many countries, there is still a need for efficient and quick testing mechanisms. These would alleviate the burden on health professionals and limit contact cases.

X-rays and CT scans have proven to be viable alternatives to the RT-PCR test for COVID-19 detection. Especially when considering (i) their availability in countries and regions where RT-PCR kits are not available, (ii) faster diagnosis time, and (iii) their reduced exposure risks.

Chung et al. [5] conducted a study on 21 symptomatic patients infected with coronavirus admitted to three hospitals in provinces of Guangdong, Jiangxi, and Shandong respectively in China from January 18th, 2020 to 27th, 2020. Their aim was to identify potential imaging features of COVID-19 from CT scans with the help of two experienced fellowship-trained cardiothoracic radiologists. The degree of lobe involvement was assessed, and a "Total Severity Score" was assigned by summing up each of the individual lobe scores. Patients were also re-evaluated to study the progression of features by the same two radiologists. Table 1 shows the common observed characteristics reported by the study. Primary observations include Ground-Glass Opacities (GGO) symptoms found in 12 patients and consolidation symptoms in 6 others. As shown in Figure 1, the virus affects more than two lobes with bilateral involvement in most cases. Other observations include rounded morphology detected in 7 patients, reticulation in 3, and crazy paving in 4 [5].

**Table 1**

Findings from Chest CT Examination in 21 Patients [5].

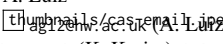
Finding	Value
Ground-glass opacities and consolidation	
Absence of both glass opacities and Consolidation	3 (14%)
Presence of either ground-glass opacities or consolidation	18 (86%)
Presence of ground-glass opacities without consolidation	12 (57%)
Presence of ground-glass opacities with consolidation	6 (29%)
Presence of consolidation without ground-glass opacities	0 (0%)
More than two lobes affected	15 (71%)
Total lung severity score	
Mean	9.9
Range	0-19


One obvious limitation of this study is the relatively low number of patients, with only 8 out of 21 carrying a follow-up CT scan. As this study was conducted during the dawn of coronavirus, this number is certainly a very respected amount. The study also shows it is feasible, by looking at chest medical imagery, to identify traits that highly indicate the presence of COVID-19. This conclusion has been reinforced by medical practice.

A systematic literature review with meta-analysis of the imaging features of COVID-19 also observed similar lung characteristics such as GGO's from patients diagnosed with

\*H. Ragab

\*\*A. Luiz

 [h.h.ragab@hw.ac.uk](mailto:h.h.ragab@hw.ac.uk) (H. Ragab); [k.k.karim@hw.ac.uk](mailto:k.k.karim@hw.ac.uk) (K. Karim); [h.batatia@hw.ac.uk](mailto:h.batatia@hw.ac.uk) (H. Batatia)

 <https://researchportal.hw.ac.uk/en/persons/hadj-batatia> (H. Batatia)

ORCID(S): 0000-0003-0433-2152 (H. Batatia)

**Table 2**

Chest X-ray imaging characteristics from multiple studies.

Study	Ground-Glass Opacities (GGO)
Huang et al. [12]	29.3%
Chen et al. [3]	14.1%
Wang et al. [28]	100.0%
Liu et al. [17]	40.1%
Chang et al. [2]	46.2%
Pan et al. [21]	22.2%
Zhang et al. [33]	77.8%

COVID-19 from multiple studies [24]. Its findings are summarized in Table 2. We observe that GGO is a common symptom among COVID-19 patients. An example being Wang et al. [28] whose study identified GGO's in 100% of the patients under examination. Another study from Zhang et al. [33] also observe GGO's in majority of the patients (77.8%).

Deep learning can be used to detect objects and patterns in images with high accuracy. As such, it can also be used to detect COVID-19 from X-ray scans by identifying related patterns. We propose a deep learning model that can analyze chest X-rays and detect presence of COVID-19 infections. Our model achieves higher sensitivity and specificity than the RT-PCR test. Furthermore, we provide heatmap images to identify areas of concern or interest for human experts.

While achieving higher diagnosis performance, the proposed solution has the advantages of being quick and affordable. It can be deployed in areas with limited medical facilities and allows telemedicine procedures. For illustration purpose, we deployed our model at [www.aiinnov.com](http://www.aiinnov.com).

The remainder of this paper is organized as follows. We review notable COVID-19 diagnosis methods based on deep learning in section 2. We introduce our deep learning-based approach in section 3. We report our experimental results and discuss their interpretability for potential usage by medical professionals in section 4. Finally, we review our work and discuss potential future extensions and improvements in section 5.

## 2. Related work

The rapid widespread of the coronavirus global pandemic across the world forced the scientific and medical community to identify alternative diagnosis mechanisms to supplement the RT-PCR test and possibly overcome its limitations. As described in the previous section, medical imagery such as X-rays and CT scans have the potential to play a vital role in combating the rising numbers by saving valuable time in diagnosis and reducing virus exposure. We will focus on X-rays, as they are most often the first imaging modality used on suspected patients, due to their wide availability in most clinics and medical facilities.

Automatic X-ray image processing is required in order to further assist medical professionals in diagnosing COVID-19. Image segmentation is a preliminary stage to delimit the lung regions of interest (ROI). This should overcome the ambiguities due to the ribs being projected onto soft tissues

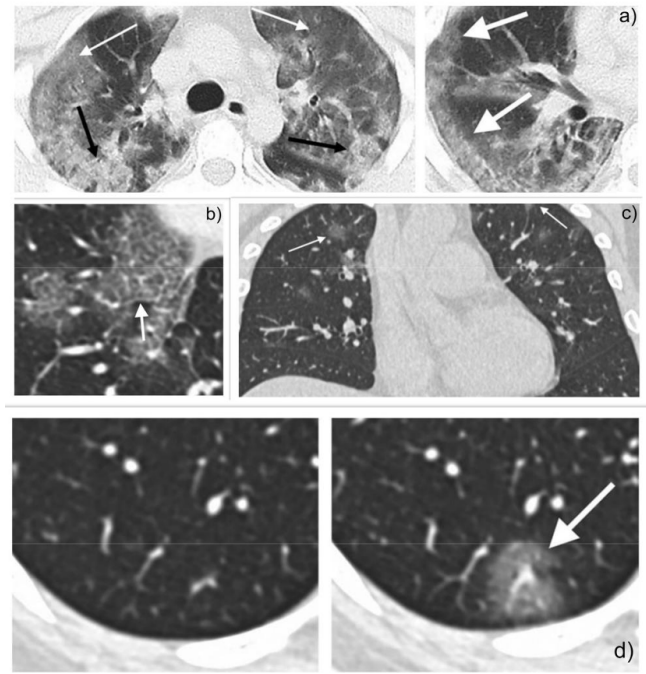


**Figure 1:** Observed lung CT Scan characteristics. a) White arrow indicates patchy GGO, and black arrow shows consolidative pulmonary opacities. b) White arrow indicates GGO's with a rounded morphology. c) White arrow shows crazy-paving pattern, GGO and interlobular septal thickening with intralobular lines. d) Follow-up CT scan progression. White arrow indicates new solitary, rounded, peripheral ground-glass lesion [5].

in such images.

### 2.1. Parsing Medical Imagery

Feeding images into classical machine learning algorithms could be challenging. Representation learning is a set of methods that allow a machine to be fed with raw data, including images, and to automatically discover the representations needed for the machine learning task at hand. Deep-learning methods are known to perform representation learning with multiple levels, obtained by composing simple but non-linear modules that each transform the representation at one level (starting with the raw input) into a representation at a higher, slightly more abstract level.

In medical image processing, using deep learning has grown very fast in recent years, with the potential of providing efficient methods for diagnosis, prognosis and follow-up that allow coping with the ever-growing volumes of medical big data [23].

X-rays have been used for various groundbreaking AI-empowered medical research applications. Deep learning techniques applied on X-ray scans have allowed scientists to detect lung cancer at an early stage. Indeed, Sim et al. conducted a multi-center study where a deep convolutional neural network (DCNN) was used to assist 12 radiologists to detect malignant pulmonary nodules on chest radiographs. The average sensitivity improved from 65.1% to 70.3% when the

radiologists re-reviewed radiographs with the DCNN software [27].

RetinaNet, a popular deep learning technique, was used for early detection of breast cancer allowing patients to have proper treatment and consequently reduce rate of morbidity [10]. Deep learning has also been used to detect both viral and bacterial Pneumonia that share similar lung characteristics with COVID-19 [16, 29].

## 2.2. COVID-19 Diagnosis using Deep Learning

Despite being the first imaging modality for patients suspected with COVID-19, X-ray images are less sensitive than 3D chest CT scans. Anomalous chest radiographs are found in 69% of the patients initially during admission and this number increases to 80% after a certain period once hospitalized [30].

Four popular deep learning architectures are used across various studies to detect the abnormalities commonly found in COVID-19 patients with lung X-ray scans, namely ResNet [32], ResNet-50 [20], ResNet-8 [14], and CNN [9, 29]. We present a few notable works from the four categories in the rest of the section.

Ghoshal et al. proposed a Bayesian CNN to estimate the uncertainty in COVID-19 prediction [9]. X-rays of 70 COVID-19 patients were obtained from Cohen et al. [6] and others from Kaggle's chest X-ray images. The authors reported that Bayesian inference improves the detection accuracy of the model from 85.7% to 92.9%.

Narin et al. experimented with three deep learning models, namely ResNet-50, InceptionV3 and Inception-ResNetV2, with the main objective of detecting COVID-19 from X-ray images [20]. Their dataset includes X-rays from 50 COVID-19 patients and 50 normal scans. The reported results indicate that the ResNet-50 model achieves the highest accuracy with 98% followed by InceptionV3 which attains 97%.

Zhang et al. also suggest a ResNet based model for COVID-19 detection [32]. Their proposed model considers COVID-19 cases as abnormal situations given a large dataset of normal X-ray images. Precisely, they experimented with a dataset containing 70 X-rays from COVID-19 patients and 1008 normal, and report 96% accuracy but a relatively low 73.5% F1 score.

Wang et al. proposed the COVID-net, a deep CNN based model, which achieves a testing accuracy of 83.5% [29]. Their dataset includes X-rays from 45 COVID-19 positive, 931 Bacterial Pneumonia, 660 viral-pneumonia, and 1203 normal X-rays.

Karakanis et al. implemented a ResNet8 model to perform multi-class classification for COVID-19, pneumonia, and normal X-rays [14]. The X-ray dataset comprised of 175 COVID-19, 100 normal, and 100 pneumonia scans. The model achieved competitive performance with 98.3% accuracy, 99.3% sensitivity and 98.1% specificity.

Table 3 summarizes the results obtained by the studies discussed in this section. They all aimed at detecting COVID-19 cases while discriminating them from Pneumonia. Despite the good results reported, the major limitation relates

to the low number of COVID-19 cases included in the experiments. Therefore, generalizability and stability of the proposed models are yet to be evaluated.

## 3. Our Approach

We propose a multiclass classifier that can categorize an X-Ray as either containing COVID-19, Pneumonia, or a healthy chest. Our classifier uses a deep learning DenseNet121 architecture [13]. The motivation of using this architecture arises from the complex nature of X-ray images that exhibit multiple tissue layers and anatomic structures projected into the 2D image.

Our hypothesis is that reusing features from different network layers allows capturing characteristic COVID-19 patterns from layered lung tissues. Architectures such as CNN do not allow such reuse of features from different layers. DenseNet121 is precisely designed for this purpose. It allows features propagation and reuse. Therefore, it is best suited given our objective.

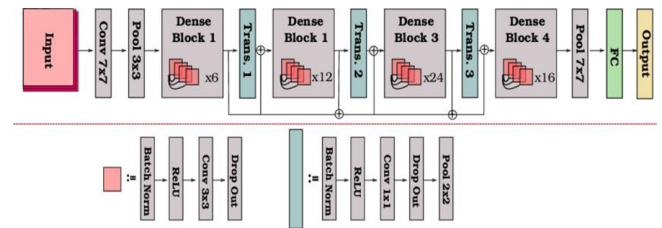


Figure 2: Architecture of DenseNet121 [22].

Figure 2 depicts the architecture of a DenseNet121 with 5 layers. Its main characteristic is the direct connections between all of them. In addition, DenseNet121 requires fewer parameters when compared to an equivalent traditional CNN. We implemented the ADAM optimization algorithm for training the model. We review our X-Ray dataset in 3.1, present our methodology in 3.2, and discuss how used transfer learning in 3.3.

### 3.1. X-ray Dataset Preparation

Our model was trained and tested using images from a Kaggle dataset<sup>1</sup>. The dataset is compiled from multiple sources [8, 18, 4]. It is an open-source database of COVID-19 cases which includes X-ray and CT scans. It includes COVID-19 and Pneumonia cases as well as healthy chest scans.

Furthermore, given the objective of our classification task to identify COVID-19 patterns, only the posterior-anterior view of the lungs was considered for training and testing. Indeed, this view visualizes lungs, bony thoracic cavity, mediastinum, and great vessels [19]. This choice allowed us to reduce the number of training instances and work with a less unbalanced dataset. Figure 3 contains the images and shows their corresponding labels.

<sup>1</sup>Available at <https://www.kaggle.com/prashant268/chest-xray-covid19-pneumonia>

**Table 3**

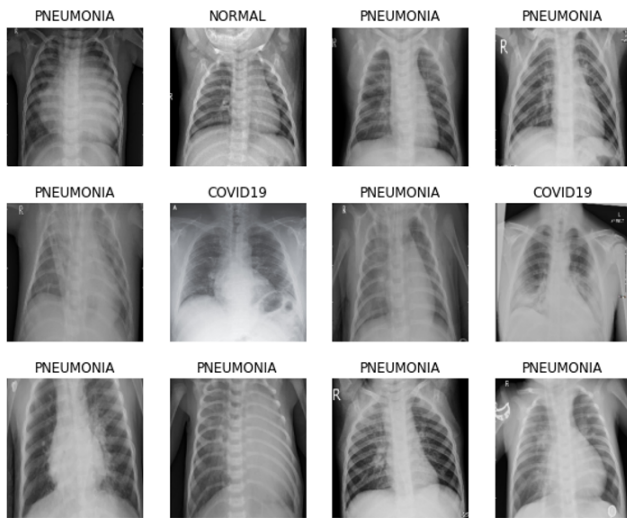
X-ray image segmentation techniques in COVID-19 diagnosis applications [26]

Proposal	Method	COVID-19	Bacterial Pneumonia	Viral Pneumonia	Normal	Accuracy	Sensitivity	Specificity	F1 Score
Ghoshal [9]	CNN	70	-	-	-	92.9%	85.7%	99.4%	75.0%
Zhang [32]	ResNet	70	-	-	1008	96.0%	96.0%	70.7%	73.5%
Narin [20]	ResNet50	50	-	50	-	98.0%	91.8%	96.6%	83.5%
Wang [29]	CNN	45	931	660	1203	83.5%	91.0%	99.5%	94.7%
Karakanis [14]	ResNet8	175	100	-	100	98.3%	99.3%	98.1%	99.1%

**Table 4**

Dataset used in our study.

Disease	Total Images	Non-augmented Training	Augmented Training	Test (not-augmented)	Unseen Data
COVID-19	572	468	1070	52	52
Pneumonia	572	468	1070	52	52
Normal	572	468	red1070	52	52

**Figure 3:** Sample of X-ray scans with labels for model training.

### 3.2. Methodology

We plan to use 10-fold cross validation and leave an eleventh fold to test the 10 models on it as unseen data. Indeed, 10-fold cross validation produces 10 models that, collectively, saw all the training dataset. The original Kaggle dataset contained 575 COVID-19 cases, 4273 Pneumonia cases, and 2583 Negatives. We built a balanced dataset of 572 samples of each of the classes (572 is a multiple of 11). The size of the eleventh fold, to which we refer to from now on as *unseen data*, is 52.

At each of the 10 iterations of the 10-fold cross validation, we take 10% of the dataset out to be used as testing dataset. The remaining 90% undergoes an augmentation step. The augmentation step uses three operators to produce slightly modified image, namely rotation, zooming and shearing. Images rotation rotates an image by 5°. Zooming applies a +2% zoom. Shearing, which distorts an image along an axis (essentially converting rectangles into parallelograms), applies a 2° counter-clockwise distortion. The augmentation of each of the 468 samples of each class (90%

**Table 5**

Results of our approach

Class	COVID-19	Normal	Pneumonia
Sensitivity	97.7%	92.7%	93.5%
Specificity	98.9%	96.8%	96.3%
F1 Score	97.7%	93.1%	93.0%

of 520) resulted in creating 1070 samples of that class. Since we have three classes, COVID-19, Pneumonia and Negatives, the total number of samples in the final training dataset is of 3210. Only the training dataset was augmented; no augmentation was applied to the test dataset. Table 4 shows the size of the data we used.

### 3.3. Training and transfer learning

Transfer learning is a machine-learning technique where a model trained for an application with some dataset is reused on another dataset. The pre-trained model approach to transfer learning consists of using the source model as a starting point for training the target model.

In order to reduce training-time and improve accuracy, we adopted the pre-trained transfer learning approach. We used an ImageNet model trained with large volume of images for classification tasks. Using the pre-trained model, we trained only the final layer. All other layers used fixed weights obtained from the prior training using the ImageNet dataset.

We implemented our deep learning solution using the Keras framework. We utilized several functions from the Callback API to control the training stage. We particularly used them for monitoring the loss metric, assessing the evolution of the learning rate to avoid plateau phenomena, and selecting models with the best performance. Practically, this led to significantly reducing the training time.

## 4. Results

Table 5 shows the results of applying our method on the dataset we described in 3.1. The table reports class-wise



**Table 6**

Comparison of the results of our approach with and without Data Augmentation.

	With Augmentation	Without Augmentation
Accuracy	94.6%	93.84%
Sensitivity	94.6 %	94.0%
Specificity	97.3 %	96.0%

**Table 7**

Comparison of our approach with RT-PCR and CNN.

Metric	Our Approach	RT-PCR	CNN	Narin et al. [20]
Accuracy	98.5%	-	93.9%	97.0%
Sensitivity	97.7%	84.2%	85.2%	91.1%
Specificity	98.9%	98.9%	98.2%	99.7%

sensitivity, specificity and F1-scores. Our cross validation resulted is 94.6% average accuracy on the balanced dataset.

Furthermore, each of the 10 models were saved after cross validation and tested on completely unseen data that were not part of the 10 folds used in cross-validation. Table 6 compares the performance of our model when augmentation is not used to when we use it. It is trivial that augmentation leads to better performance.

### Comparison to Existing Approaches

We compared the results given by our model, only for the COVID-19 class, with the RT-PCR test according to the study conducted by the Infectious Diseases Society of America (IDSA). We also did implement a CNN-based model, on the same dataset, to compare our model with deep learning models that use state of the art techniques. Furthermore, we did apply the approach proposed by Narin et al. [20] to our dataset. We contacted the authors of [14] and [32] asking for their source codes but did not get them.

Table 7 summarizes the comparison and uses three metrics, namely sensitivity, specificity and accuracy (relatively to the COVID-19 class). The table shows the high quality of our model. It can be noted that our method scores higher than RT-PCR and better than CNN. The difference is more significant for the accuracy, in favor of our method.

## 5. Discussion and Interpretation

Deep learning models are often regarded as black boxes. Interpretability and understandability of such models are needed to comprehend or discern their functioning and results. Interpretability becomes a requirement when deep learning is applied to science and medicine. In our study, we investigated means of understanding the reasoning underlying diagnosis of COVID-19 given by our model.

One way of achieving interpretability is by providing radiologists with means to cross-check their traditional distinct features obtained from lung image segmentation. For example, superpose a visualization of the output of a deep learning outcome on the original figure features (such as the GGO in Figure 1).

Various interpretation methods exist for deep-learning. For example, saliency methods are a set of tools used to analyze deep learning results [1]. Despite having been criticized due to their lack of reliability, they can provide analysts with insights about their models [15]. The most used saliency tools include i) *Saliency Map* which estimates specific parts of the image that contribute to highest layer activation [31]; ii) *Class Activation Mapping* (CAM) which averages and adds the activations of each feature map (Global Average Pooling) and uses this to highlight important regions [34]; and iii) *Gradient-Weighted CAM* (Grad-CAM) which consists in calculating the gradient of the classification score with respect to the convolutional features [25].

We calculated the Grad-CAM heatmaps of the COVID-19 class. Grad-CAM heatmaps should highlight regions in the lungs which, as discussed in section 1, exhibit the most common characteristics in patients diagnosed with COVID-19. These include features such as GGO's, consolidations, lesions, and crazy-paving patterns, which are some of the most contributing features to diagnosis. This technique provides interpretation means that would assist radiologists in identifying the same lung characteristics as with traditional segmentation-based methods.

### Grad-CAM Heat Maps for COVID-19

For the purpose of building a more interpretable model, we generated heatmaps of the COVID-19 scans. The heatmaps highlight the regions that led to the classification by our model. Heatmaps obtained for a sample of 15 previously unseen scans is displayed in Figure 4. Regions in red are the most influential in making the decision, whereas blue regions are the least influential.

We verified that the heat maps we obtained correspond to the regions highlighted from studies conducted by Harmon et al. [11] and Li et al. [16]. The lower lung lobes seem to be the most affected in patients diagnosed with COVID-19, this correlates with the observations from Chung et al. [5] and therefore, provides additional validation that lung characteristics such as GGO's, consolidations, and lesions are major contributing factors to COVID-19 detection.

To further verify that the heatmaps produced by the model are in conformance with the same observed characteristics, we have provided a subset of five X-rays scans to two senior radiologists and asked them to highlight the critical regions and provide their diagnosis results.

Figure 5 compares the radiologist's annotations and diagnosis with those produced by our model along with the heatmap result. We can observe that the heatmaps are in direct compliance with the radiologists' findings. Precisely, visually, the heatmaps show that our predictive model highlights at least one or more of the critical regions identified by the radiologist. Furthermore, all areas highlighted by the radiologist are shades of either red or purple, but never blue. We can conclude that if the model is integrated into a seamless COVID-19 or Pneumonia diagnosis workflow in which X-Ray scans are overlayed with our heatmaps, then we could considerably increase the efficiency and effectiveness of di-

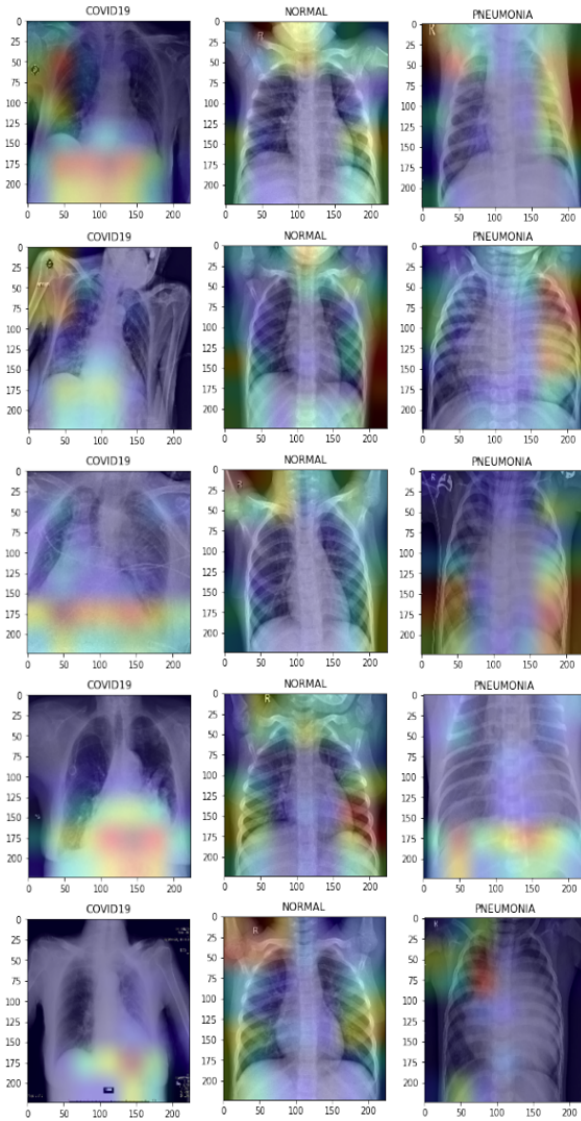


**Figure 4:** Heat map visualization for DenseNet121 results.

agnosis due to faster processing and affirmation for the results obtained.

## 6. Conclusion

The use of machine and deep learning methods in medicine has a great potential. It is the means to achieve predictive and personalized medicine, which is the next paradigm shift in the domain. This paper builds on results from many prior studies and presents a case for predictive medicine in COVID-19. It proposes a deep learning model for COVID-19 diagnosis based on X-ray images. More specifically, the proposed classification model detects lung patterns that are characteristics of COVID-19 infections using X-ray images.

The proposed model is based on the DenseNet121 architecture and was trained on a dataset from trustworthy public datasets. It consists of balanced dataset composed of 1716 images from patients with COVID-19, Pneumonia and Normal scans. Experimental results gave 94.6% accuracy, show-

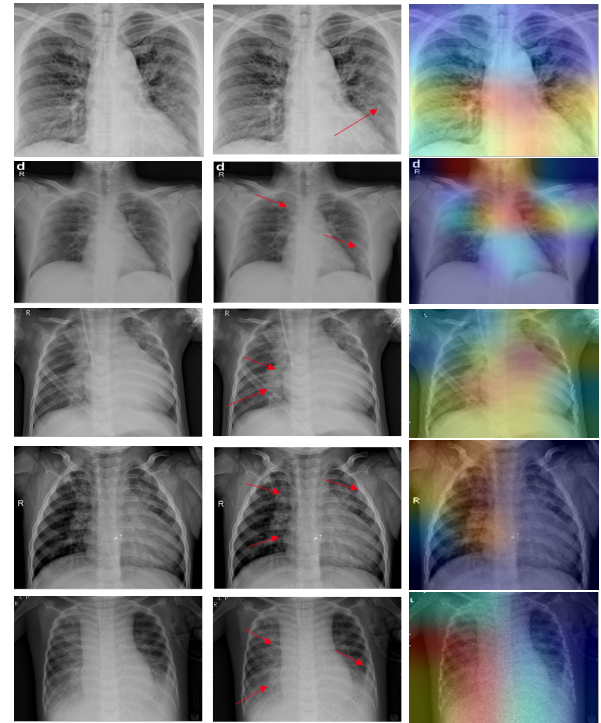


**Figure 5:** Comparison of radiologist's annotations and heatmap results. Annotations are in accordance with our classification. One can also notice the good overall matching of radiologist's annotation with high heat areas. The upper two rows correspond to COVID-19 and the lower three to pneumonia.

ing better performance than the RT-PCR and CNN-based classification methods.

We discussed our results and used interpretability techniques for understanding the underlying decisions. More specifically, salient maps were used to highlight regions in the lungs which exhibit the most common characteristics of COVID-19. We also implemented heatmaps visualization to illustrate the regions of lungs that contributed the most to the classification decision.

The proposed method is non-invasive, quick, cost effective and can lead to semi-automated telemedicine procedures. Future work will be twofold. First, a large-scale clinical study will be implemented to validate the results and derive a medical protocol for routine clinics. Second, the method will be generalized to COVID-19 CT images. The objective will be to derive prognosis using short time series of CT images. Perspective work consists also in ensuring robustness of the proposed model. One possible approach is to assess the quality of input images based on criteria to be defined.

## Acknowledgement

The authors thank Dr. G.R. Mahadevan (MD, IDCCM, D.Diab, Specialist in COVID-19) from Maya Nursing Home, Tamil Nadu for annotating the X-ray images.

## References

- [1] Adebayo, J., Gilmer, J., Muelly, M., Goodfellow, I., Hardt, M., Kim, B., 2018. Sanity checks for saliency maps. *arXiv preprint arXiv:1810.03292*.
- [2] Chang, D., Lin, M., Wei, L., Xie, L., Zhu, G., Cruz, C.S.D., Sharma, L., 2020. Epidemiologic and clinical characteristics of novel coronavirus infections involving 13 patients outside wuhan, china. *Jama* 323, 1092–1093.
- [3] Chen, N., Zhou, M., Dong, X., Qu, J., Gong, F., Han, Y., Qiu, Y., Wang, J., Liu, Y., Wei, Y., et al., 2020. Epidemiological and clinical characteristics of 99 cases of 2019 novel coronavirus pneumonia in wuhan, china: a descriptive study. *The lancet* 395, 507–513.
- [4] Chung, A.G., . Open source covid-19 dataset. URL: <https://github.com/agchung>.
- [5] Chung, M., Bernheim, A., Mei, X., Zhang, N., Huang, M., Zeng, X., Cui, J., Xu, W., Yang, Y., Fayad, Z.A., et al., 2020. Ct imaging features of 2019 novel coronavirus (2019-ncov). *Radiology* 295, 202–207.
- [6] Cohen, J.P., Morrison, P., Dao, L., Roth, K., Duong, T.Q., Ghassemi, M., 2020. Covid-19 image data collection: Prospective predictions are the future. *arXiv preprint arXiv:2006.11988*.
- [7] Elflein, J., 2021. Covid-19 tests by country. URL: <https://www.statista.com/statistics/1028731/covid19-tests-select-countries-worldwide/>.
- [8] Ganglia, B., . Covid-19 image data collection. URL: <https://github.com/ieee8023/covid-chestxray-dataset>.
- [9] Ghoshal, B., Tucker, A., 2020. Estimating uncertainty and interpretability in deep learning for coronavirus (covid-19) detection. *arXiv preprint arXiv:2003.10769*.
- [10] Hamed, G., Marey, M.A.E.R., Amin, S.E.S., Tolba, M.F., 2020. Deep learning in breast cancer detection and classification, in: *Joint European-US Workshop on Applications of Invariance in Computer Vision*, Springer. pp. 322–333.
- [11] Harmon, S.A., Sanford, T.H., Xu, S., Turkbey, E.B., Roth, H., Xu, Z., Yang, D., Myronenko, A., Anderson, V., Amalou, A., et al., 2020. Artificial intelligence for the detection of covid-19 pneumonia on chest ct using multinational datasets. *Nature communications* 11, 1–7.
- [12] Huang, C., Wang, Y., Li, X., Ren, L., Zhao, J., Hu, Y., Zhang, L., Fan, G., Xu, J., Gu, X., et al., 2020. Clinical features of patients infected with 2019 novel coronavirus in wuhan, china. *The lancet* 395, 497–506.
- [13] Huang, G., Liu, Z., Van Der Maaten, L., Weinberger, K.Q., 2017. Densely connected convolutional networks, in: *Proceedings of the IEEE conference on computer vision and pattern recognition*, pp. 4700–4708.
- [14] Karakanis, S., Leontidis, G., 2021. Lightweight deep learning models for detecting covid-19 from chest x-ray images. *Computers in Biology and Medicine* 130, 104181.
- [15] Kindermans, P.J., Hooker, S., Adebayo, J., Alber, M., Schütt, K.T., Dähne, S., Erhan, D., Kim, B., 2019. The (un) reliability of saliency methods, in: *Explainable AI: Interpreting, Explaining and Visualizing Deep Learning*. Springer. pp. 267–280.
- [16] Li, L., Qin, L., Xu, Z., Yin, Y., Wang, X., Kong, B., Bai, J., Lu, Y., Fang, Z., Song, Q., et al., 2020. Artificial intelligence distinguishes covid-19 from community acquired pneumonia on chest ct. *Radiology*.
- [17] Liu, K., Fang, Y.Y., Deng, Y., Liu, W., Wang, M.F., Ma, J.P., Xiao, W., Wang, Y.N., Zhong, M.H., Li, C.H., et al., 2020. Clinical characteristics of novel coronavirus cases in tertiary hospitals in hubei province. *Chinese medical journal*.
- [18] Mooney, P., 2018. Chest x-ray images (pneumonia). URL: <https://www.kaggle.com/paultimothymooney/chest-xray-pneumonia>.
- [19] Murphy, K., Smits, H., Knoop, A.J., Korst, M.B., Samson, T., Scholten, E.T., Schalekamp, S., Schaefer-Prokop, C.M., Philipsen, R.H., Meijers, A., et al., 2020. Covid-19 on chest radiographs: a multireader evaluation of an artificial intelligence system. *Radiology* 296, E166–E172.
- [20] Narin, A., Kaya, C., Pamuk, Z., 2020. Automatic detection of coronavirus disease (covid-19) using x-ray images and deep convolutional neural networks. *arXiv preprint arXiv:2003.10849*.
- [21] Pan, Y., Guan, H., Zhou, S., Wang, Y., Li, Q., Zhu, T., Hu, Q., Xia, L., 2020. Initial ct findings and temporal changes in patients with the novel coronavirus pneumonia (2019-ncov): a study of 63 patients in wuhan, china. *European radiology* 30, 3306–3309.
- [22] Radwan, N., 2019. Leveraging sparse and dense features for reliable state estimation in urban environments. Ph.D. thesis. University of Freiburg, Freiburg im Breisgau, Germany.
- [23] Razzak, M.I., Naz, S., Zaib, A., 2018. Deep learning for medical image processing: Overview, challenges and the future. *Classification in BioApps*, 323–350.
- [24] Rodriguez-Morales, A.J., Cardona-Ospina, J.A., Gutiérrez-Ocampo, E., Villamizar-Peña, R., Holguin-Rivera, Y., Escalera-Antezana, J.P., Alvarado-Arnez, L.E., Bonilla-Aldana, D.K., Franco-Paredes, C., Henao-Martinez, A.F., et al., 2020. Clinical, laboratory and imaging features of covid-19: A systematic review and meta-analysis. *Travel medicine and infectious disease* 34, 101623.
- [25] Selvaraju, R.R., Cogswell, M., Das, A., Vedantam, R., Parikh, D., Batra, D., 2017. Grad-cam: Visual explanations from deep networks via gradient-based localization, in: *Proceedings of the IEEE international conference on computer vision*, pp. 618–626.
- [26] Shi, F., Wang, J., Shi, J., Wu, Z., Wang, Q., Tang, Z., He, K., Shi, Y., Shen, D., 2020. Review of artificial intelligence techniques in imaging data acquisition, segmentation and diagnosis for covid-19. *IEEE reviews in biomedical engineering*.
- [27] Sim, Y., Chung, M.J., Kotter, E., Yune, S., Kim, M., Do, S., Han, K., Kim, H., Yang, S., Lee, D.J., et al., 2020. Deep convolutional neural network-based software improves radiologist detection of malignant lung nodules on chest radiographs. *Radiology* 294, 199–209.
- [28] Wang, D., Hu, B., Hu, C., Zhu, F., Liu, X., Zhang, J., Wang, B., Xi, ang, H., Cheng, Z., Xiong, Y., et al., 2020a. Clinical characteristics of 138 hospitalized patients with 2019 novel coronavirus-infected pneumonia in wuhan, china. *Jama* 323, 1061–1069.
- [29] Wang, L., Lin, Z.Q., Wong, A., 2020b. Covid-net: A tailored deep convolutional neural network design for detection of covid-19 cases from chest x-ray images. *Scientific Reports* 10, 1–12.
- [30] Wong, H.Y.F., Lam, H.Y.S., Fong, A.H.T., Leung, S.T., Chin, T.W.Y., Lo, C.S.Y., Lui, M.M.S., Lee, J.C.Y., Chiu, K.W.H., Chung, T.W.H., et al., 2020. Frequency and distribution of chest radiographic findings in patients positive for covid-19. *Radiology* 296, E72–E78.
- [31] Zeiler, M.D., Fergus, R., 2014. Visualizing and understanding convolutional networks, in: *European conference on computer vision*, Springer. pp. 818–833.
- [32] Zhang, J., Xie, Y., Li, Y., Shen, C., Xia, Y., 2020a. Covid-19 screening on chest x-ray images using deep learning based anomaly detection. *arXiv preprint arXiv:2003.12338*.
- [33] Zhang, M., Wang, X., Chen, Y., Zhao, K., Cai, Y., An, C., Lin, M., Mu, X., 2020b. Clinical features of 2019 novel coronavirus pneumonia in the early stage from a fever clinic in beijing. *Zhonghua jie he hu xi za zhi= Zhonghua jiehe he huxi zazhi= Chinese journal of tuberculosis and respiratory diseases* 43, 215–218.
- [34] Zhou, B., Khosla, A., Lapedriza, A., Oliva, A., Torralba, A., 2016. Learning deep features for discriminative localization, in: *Proceedings of the IEEE conference on computer vision and pattern recognition*, pp. 2921–2929.